Nuclear Engineering and Technology 55 (2023) 3071–3079

Contents lists available at ScienceDirect

Nuclear Engineering and Technology

journal homepage: www.elsevier.com/locate/net

Original Article

A surrogate model for the helium production rate in fast reactor MOX fuels

D. Pizzocri, M.G. Katsampiris, L. Luzzi*, A. Magni, G. Zullo

Politecnico di Milano, Department of Energy, Nuclear Engineering Division, Via La Masa 34, 20156, Milano, Italy

ARTICLE INFO

Article history:
Received 26 January 2023
Received in revised form
18 April 2023
Accepted 29 April 2023
Available online 7 May 2023

Keywords:
MOX fuel
Minor actinides
Helium production
SCIANTIX
Generation IV fast reactors

ABSTRACT

Helium production in the nuclear fuel matrix during irradiation plays a critical role in the design and performance of Gen-IV reactor fuel, as it represents a life-limiting factor for the operation of fuel pins. In this work, a surrogate model for the helium production rate in fast reactor MOX fuels is developed, targeting its inclusion in engineering tools such as fuel performance codes. This surrogate model is based on synthetic datasets obtained via the SCIANTIX burnup module. Such datasets are generated using Latin hypercube sampling to cover the range of input parameters (e.g., fuel initial composition, fission rate density, and irradiation time) and exploiting the low computation requirement of the burnup module itself. The surrogate model is verified against the SCIANTIX burnup module results for helium production with satisfactory performance.

1. Introduction

Developments in research regarding Generation IV fast reactors with minor actinide (MA)-bearing MOX fuel, and the related fuel cycle technologies dictate a need for a detailed understanding of fuel behavior under irradiation as well as under storage conditions. One important aspect of the behavior of MA-bearing MOX fuel is the helium production in the fuel itself, and the potential helium release into the fuel rod free volume increasing fuel pin internal pressure [1]. When MAs are included in the fuel initial composition in comparison with conventional uranium-plutonium oxide or uranium dioxide fuel, a considerable contribution to the helium production rate arises from these short-lived α-decaying nuclides. A second path to produce helium in nuclear fuel is the ^{16}O (n,α) reaction, which is progressively more relevant under faster neutron spectra [1]. The third and last path for helium production in nuclear fuel are ternary fissions, with MA isotopes having relatively higher helium yield from fast fissions compared to uranium and plutonium isotopes [2]. Depletion codes are the standard tools applied to predict helium production following these production paths. They enable a reliable estimation of the concentration evolution of the actinides contained within the fuel by considering the sequential steady state neutronics solution at each burnup step. The ORIGEN2 code is a point-depletion and radioactive decay software used in simulating nuclear fuel cycles and calculating the nuclide compositions and characteristics of materials contained therein [3]. Monteburns is a tool integrating the Monte-Carlo code MCNP with ORIGEN2 in a fully automatic way, enabling depletion calculations [4]. The SCALE-4 modular code is used for depletion and criticality calculations in light water reactors (LWR), while recently, Xia and co-authors released MODEC, a depletion code specific to molten salt reactors calculations [5,6]. Romano and co-authors released OpenMC [8], an open-source, high-fidelity Monte-Carlo code allowing for solid geometry and continuous energy calculations, which was coupled by de Troullioud de Lanversin and co-authors [7] with the ONIX depletion code, to provide one-group cross section data.

* Corresponding author.
E-mail address: lelio.luzzi@polimi.it (L. Luzzi).

https://doi.org/10.1016/j.net.2023.04.044

Fuel performance codes, dedicated to thermo-mechanical analysis of fuel pins, typically employ less computationally expensive approaches compared to depletion codes ([9,10]) to estimate helium production rates. These codes use either dedicated burnup modules, directly solving the Bateman equations but with greatly simplified approaches towards cross sections,[1] e.g., the TUBRNP module of the codes TRANSURANUS [11] and FRAPCON [12], RAPID [13], RTOP [14], and the burnup module embedded in the DIONISIO code [15], or correlations directly calculating the helium production rate from a set of input parameters. Regarding helium production correlations, Akie and co-authors [16] proposed a simple mechanistic formula for helium production which considers the three aforementioned main pathways of helium production inside the fuel, verified it with the high-fidelity results of the SWAT code, and validated it against experimental data produced at the JOYO fast reactor. Recently, Tarasov and co-authors [17] modified the BONUS model to describe helium and hydrogen behavior in irradiated fuels and implemented it in the MFPR/R, SFPR and BERKUT-U codes. Either of these two approaches to calculate helium production has its respective advantages and disadvantages: (1) burnup modules have greater accuracy at the expense of an increased computational cost, whereas (2) stand-alone correlations are specific to certain fuel/reactor combinations [18], but fast running and inherently numerically stable.

In this work, we propose the use of a fast-running burnup module to construct synthetic datasets on which a surrogate model for helium production is trained. The envisaged surrogate model is targeted to have a computational cost comparable with that of a correlation and an accuracy in line with the requirements of engineering tools such as fuel performance codes [19–21]. This methodology represents a typical application of surrogate models which is widely used in other fields [22] and is herein proposed for fuel performance. The SCIANTIX burnup module [23,24] is firstly extended leveraging high-fidelity criticality results from the SERPENT Monte Carlo code [25] to generate macroscopic cross-section lookup tables for two relevant fuel/reactor combinations, a sodium cooled fast reactor (SFR) and a lead bismuth eutectic-cooled fast reactor (LBE-FR) [26–29] and is then verified against high-fidelity depletion results for the a single fuel pin with cylindrical geometry. The extended burnup module is then used to generate synthetic datasets covering a wide range of initial compositions of MA-bearing fuel and irradiation conditions, and a surrogate model for the helium production rate is developed based on non-linear multivariate regression performed on the datasets. A schematic representation of the two aforementioned methodologies is reported in Figures A.3 and A.4 of the Appendix section.

2. Extension of the SCIANTIX burnup module

The SCIANTIX burnup module accounts for helium production via three main routes: (n,α) reactions on ^{16}O, α-decays of short-lived transuranic elements and ternary fissions. The resulting equation for the helium production rate in the SCIANTIX burnup module is thus:

$$\begin{aligned}\frac{\mathrm{d}\left[^4\mathrm{He}\right]}{\mathrm{d}t} = &\lambda_{\alpha,^{234}\mathrm{U}}\left[^{234}\mathrm{U}\right] + \lambda_{\alpha,^{235}\mathrm{U}}\left[^{235}\mathrm{U}\right] + \lambda_{\alpha,^{236}\mathrm{U}}\left[^{236}\mathrm{U}\right] + \\ &\lambda_{\alpha,^{238}\mathrm{U}}\left[^{238}\mathrm{U}\right] + \lambda_{\alpha,^{237}\mathrm{Np}}\left[^{237}\mathrm{Np}\right] + \lambda_{\alpha,^{238}\mathrm{Pu}}\left[^{238}\mathrm{Pu}\right] + \\ &\lambda_{\alpha,^{239}\mathrm{Pu}}\left[^{239}\mathrm{Pu}\right] + \lambda_{\alpha,^{240}\mathrm{Pu}}\left[^{240}\mathrm{Pu}\right] + \lambda_{\alpha,^{242}\mathrm{Pu}}\left[^{242}\mathrm{Pu}\right] + \\ &\lambda_{\alpha,^{241}\mathrm{Am}}\left[^{241}\mathrm{Am}\right] + \lambda_{\alpha,^{243}\mathrm{Am}}\left[^{243}\mathrm{Am}\right] + \\ &\lambda_{\alpha,^{242}\mathrm{Cm}}\left[^{242}\mathrm{Cm}\right] + \lambda_{\alpha,^{243}\mathrm{Cm}}\left[^{243}\mathrm{Cm}\right] + \\ &\lambda_{\alpha,^{244}\mathrm{Cm}}\left[^{244}\mathrm{Cm}\right] + \lambda_{\alpha,^{245}\mathrm{Cm}}\left[^{245}\mathrm{Cm}\right] + \\ &\sigma_{(\mathrm{n},\alpha),^{16}\mathrm{O}}\,\phi\left[^{16}\mathrm{O}\right] + y_{TF}\dot{\mathrm{F}}\end{aligned} \tag{1}$$

where $[^{\mathrm{i}}\mathrm{X}]$ (at·m^{-3}) is the concentration of the nuclide $^{\mathrm{i}}$X, $\lambda_{\alpha,^{\mathrm{i}}\mathrm{X}}$ (s^{-1}) is the α-decay constant of the nuclide $^{\mathrm{i}}$X, $\sigma_{(\mathrm{n},\alpha),^{16}\mathrm{O}}$ (m^2) is the (n,α) reaction cross-section of ^{16}O, ϕ (neutrons m^{-2}·s^{-1}) is the local neutron flux,[2] y_{TF} is the ternary fission yield which is equal to 0.22% [30], and $\dot{\mathrm{F}}$ (fissions m^{-3}·s^{-1}) is the local fission rate density. At each time step, a two-step procedure is performed: (1) the cross-section values for each nuclear reaction type regarding all nuclides are calculated from lookup tables based on the local burnup and initial fuel composition via an interpolation algorithm, and (2) the numerical integration of the Bateman equations (covering actinide isotopes and including helium, Eq (1)) is performed via a first order implicit numerical scheme [31,32]. The SERPENT package used in this work for both the SFR and the LBE-FR simulation cases contains libraries based on JEF-2.2, JEFF-3.1, ENDF/B-VI.8 and ENDF/B-VII evaluated data files.

The methodology used in this work to extend the SCIANTIX burnup module follows a standardized development procedure for the module that was originally designed as:

1. A set of high-fidelity simulations is performed (using SERPENT) for an initial fuel composition vector, corresponding to the fuel/reactor combination under evaluation.
2. For each initial composition step e_i and each burnup step bu_i, the respective cross-section values are extracted, evaluated by the reaction rate integrals in the SERPENT simulation.
3. A $(e_i \times bu_i)$ matrix is created containing the microscopic cross-section values, with each row representing the initial enrichment steps and each column the burnup steps for each nuclide and each reaction type.
4. The matrices are implemented in the SCIANTIX burnup module as lookup tables corresponding to the relevant fuel/reactor combination.

The detailed information about the fuel/reactor combinations considered in this work (SFR and LBE-FR, representative of the Generation IV concepts being developed and of past fast reactors), together with the verification results of the extended burnup module, are collected in the Appendix.

[1] Typical hypotheses are (i) considering burnup average cross section values assessed based on a priori estimation of fuel composition evolution, and (ii) considering one energy group. The resulting average cross section values are typically adjusted to match validation results, which results in these burnup modules being fast running and reliable besides being based on strong assumptions.

[2] The local neutron flux is calculated by $\phi = \dot{\mathrm{F}}/\overline{\Sigma_f}$ where $\overline{\Sigma_f}$ (m^{-1}) is the approximated one-group macroscopic fission cross-section calculated over m-fissile nuclides as $\overline{\Sigma_f} = \sum \overline{\sigma_{f,^m\mathrm{X}}}\,[^m X]$, where $\overline{\sigma_{f,^m\mathrm{X}}}$ (m^2) is the microscopic fission cross-section of nuclide ^{m}X.

3. Development of a surrogate model for the helium production rate

In this section, we present the methodology used to develop a surrogate model to calculate helium production in nuclear fuel. The basic tool employed is the extended SCIANTIX burnup module presented in Section 2, since it is fast running and adequately accurate for the prediction of helium production in nuclear fuel [24].

3.1. Methodology

The extended SCIANTIX burnup module is used to populate several synthetic datasets with calculated helium concentration values as a function of the input variable matrix. The output vector $Y_{N,n}$ (i.e., the helium concentration) is calculated by the code as a function of a selection of n values of N input variables composing the input matrix $I_{N,n}$, sampled from predefined ranges. By examining the probability distribution of the output $Y_{N,n}(I_{N,n})$ the desired information of the dependence of helium concentration on each input variable can be obtained. The number of input variables N and number of values sampled n dictate the computational time for the development of the synthetic datasets (e.g., for the generation of a 10′000 values dataset, the computational time required is around 3 h).

To ensure that the entire distribution of each of the input variables $I_{i,n}$ is represented by input values, the Latin hypercube sampling (LHS) technique is adopted: the range of each $I_{i,n}$ is divided into M strata of equal marginal probability $1/M$ and sampled only once from each stratum [33]. Using this technique, the advantage of limiting the amount of input values per each input variable and representing them in a fully stratified manner is evident. For example, Fig. 1 reports the plutonium per heavy metal ratio, Pu/HM, input variable distribution for 881 data points, highlighting the dense coverage of values over the sampling space if compared to the same number of points obtained via a random sampling.

The input variables considered in this analysis are the initial fuel composition in terms of all constituent nuclides expressed as the ratio of each nuclide per heavy metal (^{i}X/HM), the initial oxygen to metal ratio of the fuel O/M, the initial fuel density ρ_{fuel}, the fuel temperature T_{fuel}, the irradiation time t_{irr} and the fission rate density $\dot{F}$. The sampling ranges of each variable are shown in Table 1. The limits are chosen in line with the predictive capabilities

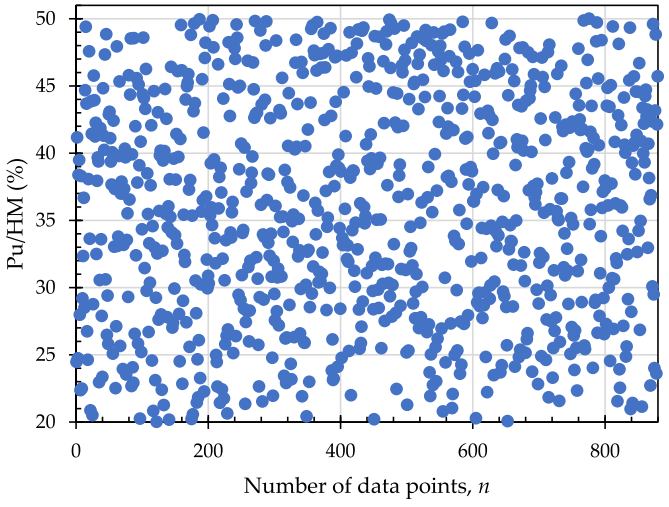

Fig. 1. Scatterplot produced using the Latin hypercube sampling technique for 881 data points of Pu/HM values as an example of an input variable coverage density.

Table 1
Ranges of the input variable values considered for the development of the helium production correlation.

Variable	Symbol	Range
Irradiation time (h)	t_{irr}	100–100′000
O/M (/)	O/M	1.95–2.00
Fission rate density (fiss·m^{-3}· s^{-1})	$\dot{F}$	$1{\cdot}10^{18}$–$1{\cdot}10^{19}$
^{235}U enrichment (at.%)	[^{235}U]	0.711–5
Pu/HM (at.%)	[Pu]	20–50
Np/HM (at.%)	[Np]	0–5
Am/HM (at.%)	[Am]	0–5
Cm/HM (at.%)	[Cm]	0–5
Fuel density (kg·m^{-3})	ρ_{fuel}	9325–10970
Average fuel temperature (K)	T_{fuel}	900–1900

of the extended SCIANTIX burnup module as well as with the fuel specifications of a selection of Generation IV reactor core concepts [29]. The implementation of the LHS technique is performed in MATLAB [34] coupled with the SCIANTIX code for the helium concentration calculation. The training dataset is composed of the input matrix $I_{N,n}$ representing the contribution of each input variable, and an output vector $Y_{N,n}$. Subsequently, multivariate nonlinear regression and statistical analysis was performed with the JMP statistical package [35] to formulate a final correlation for the two reactor cases of interest, SFR and LBE-FR. The method of stepwise regression employed is forward regression.

The regression is performed by considering the *p-values* of each regressor with respect to the output values in an iterative process. The *p-value* is defined as the probability under the assumption of no effect, or no difference (null hypothesis), of obtaining a result equal to or more extreme than what is actually observed under a defined statistical model [36]. Using this definition, each regressor is added to the surrogate model in consideration of its *p-value* being below the 0.05 threshold, i.e., a 95% of confidence on the significance of the regressor itself. The smaller the *p-value*, the greater statistical incompatibility of the data with the null hypothesis, and hence the more the regressor is needed in the surrogate model. Within this approach, collinearity between input variables is avoided by including only one of the inter-correlated variables in the final model (e.g., irradiation time and fission rate density are heavily correlated with burnup thus the latter is excluded from the final model, given also that the former two variables can be used as input in the SCIANTIX burnup module). At each iteration step, after a variable has been added to the model, the *p-values* change accordingly for each regressor.

3.2. Surrogate model

The described methodology is applied together with the aforementioned requirements and restrictions, to select two surrogate models out of the candidate models examined. one for the SFR and the LBE-FR case. Each surrogate model comprises seven dependencies:

(i) Irradiation time t_{irr} (h).
(ii) Fission rate density $\dot{F}$ (fissions m^{-3}· s^{-1}).
(iii) Total plutonium content Pu/HM (at.%).
(iv) Fuel density ρ_{fuel} (kg·m^{-3}).
(v) Initial americium-241 concentration ^{241}Am/HM (at.%).
(vi) Initial americium-242 concentration ^{242}Am/HM (at.%).
(vii) Initial curium-242 concentration ^{242}Cm/HM (at.%).

The quality of the final fit and the accuracy of the models were quantified in terms of the RMSE, the coefficient of determination R^2 and the adjusted coefficient of determination R^2_{adj} [37].The

proposed surrogate models for the SFR and the LBE-FR cases are in the form:

$$\frac{\mathrm{d}\left[^4\mathrm{He}\right]}{\mathrm{d}t_{\mathrm{irr}}} = A \cdot t_{\mathrm{irr}}^{A-1} 10^{P},$$
$$P = B \cdot \dot{\mathrm{F}} + \left(C \cdot [\mathrm{Pu}] + D \cdot [\mathrm{Pu}]^2 + E \cdot [\mathrm{Pu}]^3\right) + \quad (2)$$
$$F \cdot \rho_{\mathrm{fuel}} + G \cdot \left[^{241}\mathrm{Am}\right] + H \cdot \left[^{242}\mathrm{Am}\right] + I \cdot \left[^{242}\mathrm{Cm}\right] + S$$

where A, B, C, D, E, F, G, H, I and S are coefficients, reported in Table 2, for the two fuel/reactor combination cases along with the respective standard errors. An in-depth look at coefficient values indicates minor differences between the SFR and LBE-FR cases considered: the values and the relative weights of the coefficients in the surrogate models are similar, indicating that the dominant path of helium production are comparable in these two reactor/fuel concepts, as expected from the similar fuel and cladding compositions reported in Table A1.

Eq. (2) can be analytically solved for Log[^{4}He]. The functional dependencies on the parameters are not representative of a physical behavior but are the results of a data-driven selection among possible dependencies and are valid within the ranges reported in Table 1. The statistical method used to produce the functional form of Eq. (2) is akin to a machine learning approach, in the sense that it links inputs and outputs in a significant way without the need to incorporate an a priori physical description.

Since the proposed surrogate model is made of a single ordinary differential equation, its computational requirement is reduced compared to the use of state-of-the-art burnup modules adopted in fuel performance codes, which require the coupled solution of tens to hundreds of ordinary differential equations.

4. Validation of the surrogate model

For the development of the two surrogate models, two training datasets were generated using the LHS method on the extended SCIANTIX burnup module as discussed in Section 3.1, one for the SFR case of $n = 8538$ data points, and one for the LBE-FR case of $n = 8579$ data points. Apart from these two training datasets, five validation datasets were generated for the SFR case, and four validation datasets were generated for the LBE-FR case, with different sizes and variable limits for the purpose of assessing the predictive capability of the proposed surrogate models in a variety of different conditions. The details of each dataset are shown in Table 3. The specifications chosen for each dataset reflect possible applicative cases for the surrogate models and can be divided in three different categories: fuel composition – datasets (b), (g), (h) and (i), reactor power – dataset (c), and thermomechanical properties – dataset (e). The choice of these specific datasets for the validation of the surrogate model is done targeting specific applications in terms of reactor concepts and irradiation experiments to be simulated. The extension of the validation to other conditions is planned in the future as broader applications of the surrogate model are pursued.

The surrogate model performance for the SFR case is shown in Fig. 2. As expected, it exhibits the best performance for the training dataset (a). For the datasets (b) to (e) the surrogate model exhibits satisfactory predictive capability, particularly considering the wide applicability range in terms of irradiation conditions, with most points being concentrated around the plot diagonal, and with RMSE ranging from around 0.20 to 0.28 as shown in Table 4. The R^2 and R^2_{adj} statistic metrics range from around 0.60 to 0.71, indicating a reasonable fit of the surrogate model to the values produced from the extended SCIANTIX burnup module. Fig. 3 reports the surrogate model performance for the LBE-FR case, where the proposed surrogate model exhibits a better performance against the generated datasets compared to the SFR case (see Table 4). The variance

Table 2
Values of the coefficients in the surrogate model for the helium production rate for the two fuel/reactor combinations, with the corresponding standard error (i.e., the half-width of their respective 95% confidence interval).

Coefficient	Variable	SFR	Standard error	LBE-FR	Standard error
A	t_{irr}	$6.70\ 10^{-1}$	$3.84\ 10^{-3}$	$6.77\ 10^{-1}$	$3.75\ 10^{-3}$
B	$\dot{\mathrm{F}}$	$2.58\ 10^{-21}$	$6.05\ 10^{-23}$	$2.66\ 10^{-21}$	$5.87\ 10^{-23}$
C	[Pu]	$-9.01\ 10^{-1}$	$1.36\ 10^{-2}$	$-9.25\ 10^{-1}$	$1.31\ 10^{-2}$
D	$[\mathrm{Pu}]^2$	$2.38\ 10^{-2}$	$3.91\ 10^{-4}$	$2.44\ 10^{-2}$	$3.77\ 10^{-4}$
E	$[\mathrm{Pu}]^3$	$-2.05\ 10^{-4}$	$3.65\ 10^{-6}$	$-2.10\ 10^{-4}$	$3.51\ 10^{-6}$
F	ρ_{fuel}	$3.12\ 10^{-5}$	$3.49\ 10^{-6}$	$3.75\ 10^{-5}$	$3.38\ 10^{-6}$
G	$\left[^{241}\mathrm{Am}\right]$	$6.80\ 10^{-2}$	$3.99\ 10^{-3}$	$7.37\ 10^{-2}$	$3.78\ 10^{-3}$
H	$\left[^{242}\mathrm{Am}\right]$	$1.69\ 10^{-1}$	$3.97\ 10^{-3}$	$1.61\ 10^{-1}$	$3.87\ 10^{-3}$
I	$\left[^{242}\mathrm{Cm}\right]$	$1.85\ 10^{-1}$	$3.05\ 10^{-3}$	$1.79\ 10^{-1}$	$2.98\ 10^{-3}$
S	–	34.1	$1.58\ 10^{-1}$	34.3	$1.51\ 10^{-1}$

Table 3
Datasets generated with the extended SCIANTIX burnup module and used for training and validation of the surrogate model for the helium production rate.

Dataset	Number of data points, n	Fuel/Reactor	Specifications
(a) Training	8538	MOX/SFR	Full variable ranges
(b) Validation	10371	MOX/SFR	Cm/HM = 0 and Np/HM = 0
(c) Validation	99445	MOX/SFR	$\dot{\mathrm{F}} \leq 1.32{\cdot}10^{19}$
(d) Validation	86332	MOX/SFR	Full variable ranges
(e) Validation	9973	MOX/SFR	Constant O/M, T_{fuel}, ρ_{fuel}
(f) Training	8579	MOX/LBE-FR	Full variable ranges
(g) Validation	84648	MOX/LBE-FR	Am/HM = 0
(h) Validation	9968	MOX/LBE-FR	Constant Pu/HM = 20%
(i) Validation	313	MOX/LBE-FR	Constant Pu/HM = 50%

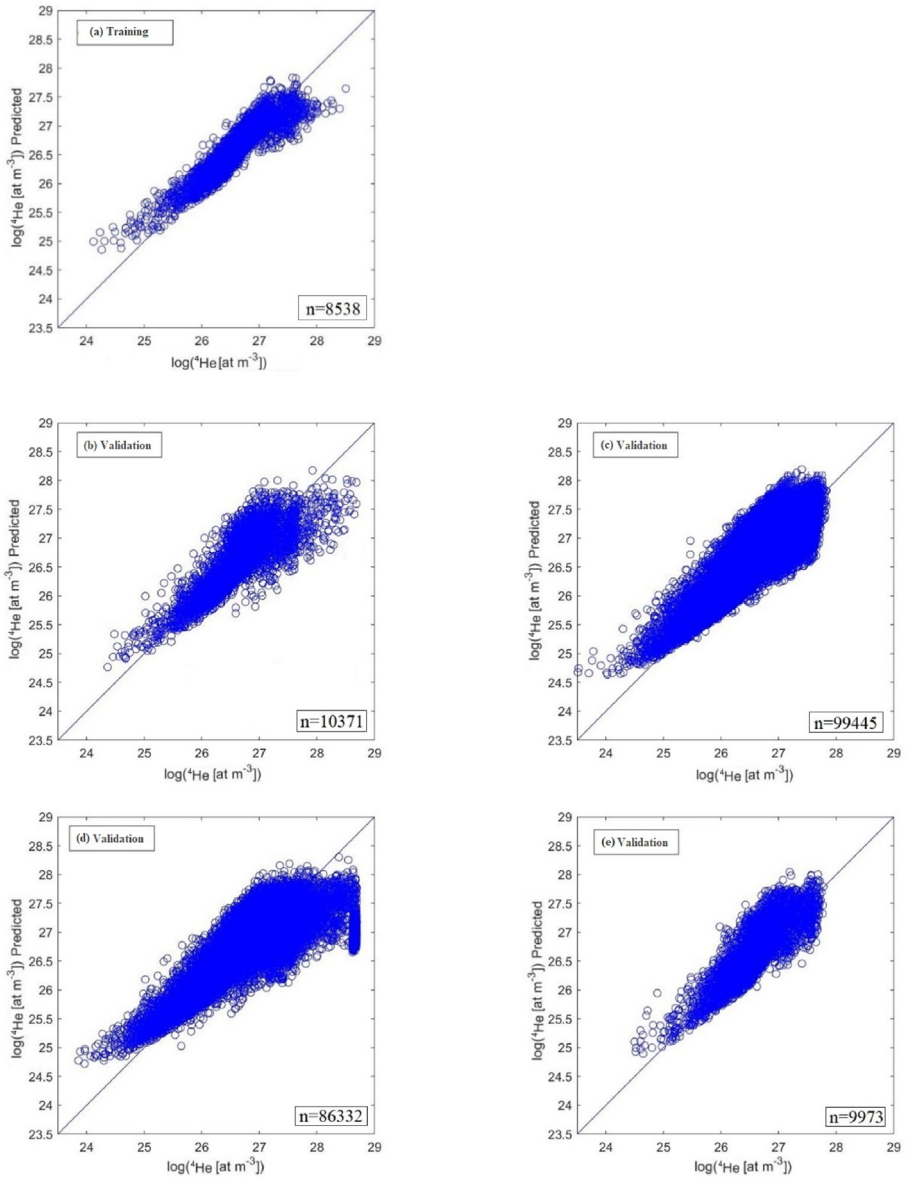

Fig. 2. Evaluation of the proposed surrogate model for the helium production rate (y-axis) against the values calculated by the SCIANTIX burnup module (x-axis) for 5 datasets in the SFR case, where (a) is the training dataset and (b) to (e) are validation datasets.

Table 4
Statistic validation metrics of the proposed surrogate model for the helium production rate for each dataset on the SFR and LBE-FR cases.

SFR case					
Dataset	(a) Training	(b)	(c)	(d)	(e)
n	8538	10371	99445	86332	9973
RMSE	0.1650	0.2759	0.1986	0.2059	0.1976
R^2	0.8123	0.6019	0.7106	0.6889	0.7085
R^2_{adj}	0.8122	0.6017	0.7104	0.6889	0.7083
LBE-FR case					
Dataset	(f) Training	(g)	(h)	(i)	
n	8579	84648	9968	313	
RMSE	0.1486	0.1504	0.1818	0.3094	
R^2	0.8441	0.8455	0.7542	0.5136	
R^2_{adj}	0.8440	0.8455	0.7540	0.5094	

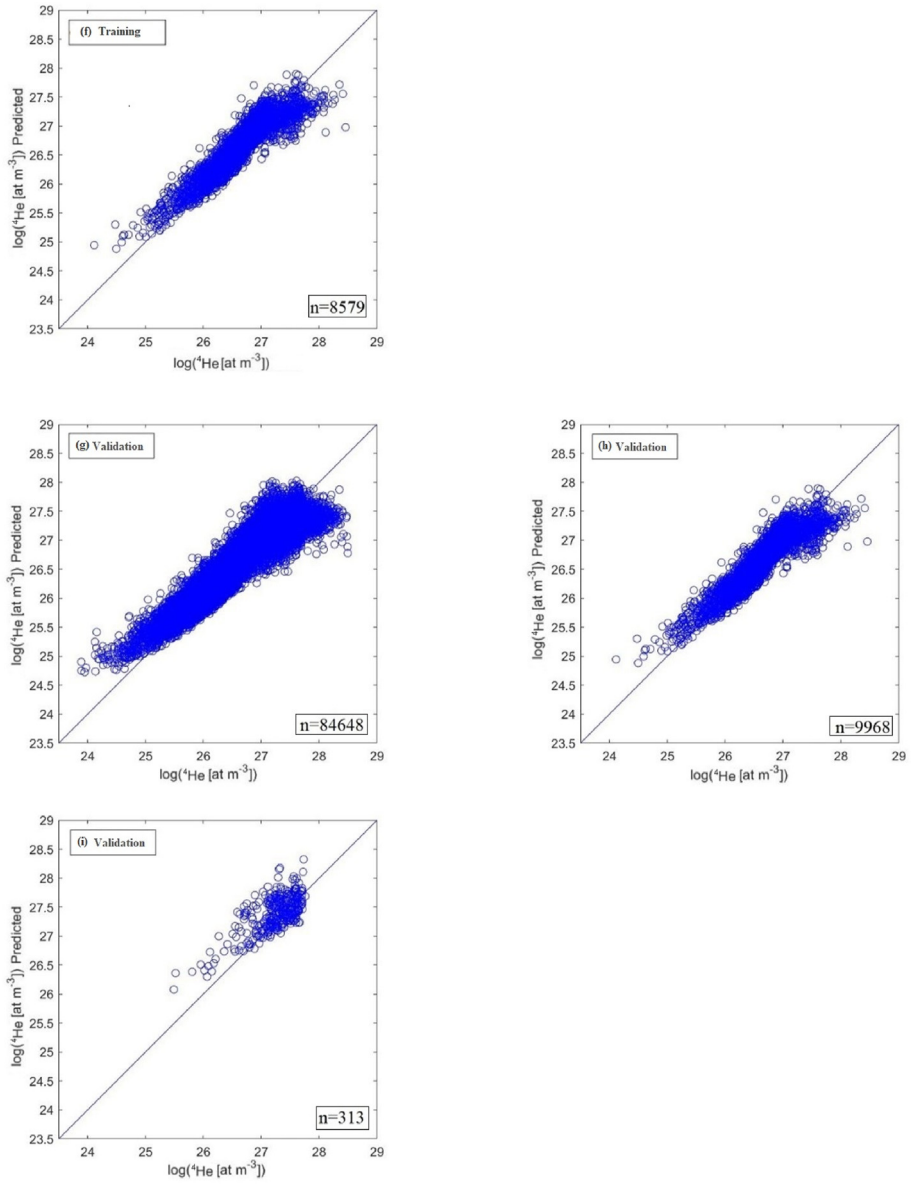

Fig. 3. Evaluation of the proposed surrogate model for the helium production rate (y-axis) against the values calculated by the SCIANTIX burnup module (x-axis) for 4 datasets in the LBE-FR case, where (f) is the training dataset and (g) to (i) are validation datasets.

associated with the predicted values occurs due to the high number of input variable combinations which lead to different burnup values for each initial fuel composition. As a general tendency, with higher number of data points in the dataset, better agreement is observed as a denser matrix of input values is generated.

5. Conclusions

The objective of this work is the development of a surrogate model for the prediction of the helium production rate. The intended use of this surrogate model is in the framework of fuel performance codes, where it aims at reducing the computational requirement of depletion calculations while providing satisfactory levels of accuracy.

Using the extended burnup module of the SCIANTIX code as a fast-running reference tool, synthetic datasets were generated with a Latin hypercube sampling technique working on several input vectors covering a wide span of initial fuel compositions and thermophysical properties correlated to the production of helium in the fuel. Non-linear multivariate regression was performed to obtain surrogate models for the helium production rate in sodium and lead-bismuth eutectic fast reactor cases. The direct use of this surrogate model allows to bypass entirely the need of a burnup module for the assessment of the helium production rate in the fuel, which is of potential interest for fuel performance codes targeting efficient thermo-mechanic calculations in the preliminary stages of the design process.

The proposed surrogate models for the helium production rate have been validated against independently generated datasets and found to be satisfactorily reliable in the considered ranges of input variables. The current version of the developed surrogate models is available in SCIANTIX. Further validation is targeted in future work, addressing other applicative conditions in which the surrogate model can be employed, and other tools, such as fuel performance codes (e.g., TRANSURANUS) coupled with SCIANTIX for the simulation of fast reactor fuel pins.

A natural extension of the proposed approach, i.e., using a fast-running reference calculation to derive surrogate model tailored to a specific irradiation experiment or a reactor case, embraces a digital twin approach. Such dedicated surrogate model can ease the development of new reactor designs, since fast running and inherently stable simulation tools are key for accelerating the design process.

Declaration of competing interest

The authors declare that they have no known competing financial interests or personal relationships that could have appeared to influence the work reported in this paper.

Acknowledgements

This work has received funding from the Euratom research and training programme 2019–2020 under grant agreement No. 945077 (PATRICIA Project).

Appendix. Extension of the SCIANTIX burnup module

We herein briefly describe the extension of the SCIANTIX burnup module (together with its verification), which has been propaedeutic to the development of the surrogate model for the helium production rate and serves as a guideline for future extensions and developments of analogous models.

The SCIANTIX burnup module interpolates cross-sections from lookup tables constructed from high-fidelity depletion calculations. These rely on SERPENT for the evaluation of the reaction rate integrals in the fuel. To obtain the absolute value of the reaction rate integrals, SERPENT considers a user-defined source normalization term. A reactor power of 40 $kW \cdot kg^{-1}$ has been assumed, corresponding to a fission rate density of $1.32 \cdot 10^{19}$ fissions $m^{-3} \cdot s^{-1}$ for the SFR case and of $1.17 \cdot 10^{19}$ fissions $m^{-3} \cdot s^{-1}$ for the LBE-FR case, with a fission energy of $3.33 \cdot 10^{-13}$ J (208 MeV). The SERPENT depletion calculation adopts the Chebyshev Rational Approximation Method (CRAM) used for the decomposition and solution of the system determined by the burnup matrix [30]. A predictor-corrector algorithm is used for each calculation node, with linear extrapolation occurring in the predictor step for time integration and linear interpolation occurring in the corrector step. An initial neutron population of 10^4 neutrons is used, with 100 active and 30 inactive cycles which facilitates reasonable computational times with relatively low standard deviation [38].

The simulation domain of the SERPENT code consists of a single fuel pin with cylindrical geometry, composed of the uniform fuel pellet, the fuel-cladding gap and the cladding, encompassed by the respective coolant material. The simulation universe is a cube of side length equal to the fuel pin length. A reflective boundary condition is applied at the end-surfaces of the defined simulation universe [38]. The specifications of the SERPENT simulation are collected in Table A1. The depletion calculation was performed in 81 equally distanced burnup steps of 2.5 GWd/t_{HM} up to 200 GWd/t_{HM} and 31 plutonium enrichment (Pu/HM) steps starting from 20 up to 51 at.%. Subsequently, the extended lookup tables of cross sections obtained from SERPENT results has been implemented in the SCIANTIX burnup module.

The predictive capabilities of the extended SCIANTIX burnup module are verified against the high-fidelity SERPENT results (Table A2 collects the characteristics of the two sets of simulations performed). The verification is performed for 31 initial enrichment steps for each of the 22 nuclides considered by the burnup module [24], and for the two fuel/reactor combination cases. A schematic representation of the verification grid used is shown in Fig. A1. The verification grid allows to test the SCIANTIX burnup module performance in correspondence of the burnup/enrichment points used to construct the lookup table and away from these points as well. Each cross-section value calculated by SERPENT corresponds to a combination of burnup and enrichment. The average RMSE for all the plutonium enrichment steps considered is shown in Fig. A2, where it is evident that the extended burnup module has a consistently better predictive performance compared to the previous version, albeit with a small gain for enrichments up to 41% where the RMSE improves significantly.

Table A1
Specifications of the SERPENT simulations for the two fuel/reactor combinations.

Parameter	MOX/SFR	MOX/LBE-FR
External pellet radius (mm)	2.71	2.71
Radial gap (mm)	0.116	0.116
U/HM (%)	80–49[a]	80–49[a]
Pu/HM (%)	20–51[b]	20–51[b]
Enrichment step width (at/HM.%)	1	1
O/M ratio	1.957	1.957
Fuel density ($kg \cdot m^{-3}$)	10970	10970
Column length (mm)	850	850
Cladding material	15-15 Ti-stabilized SS[c]	15-15 Ti-stabilized SS[c]
Cladding thickness	0.45	0.45
Cladding density ($kg \cdot m^{-3}$)	7950	7950
Coolant	Sodium	Lead-Bismuth Eutectic (Pb 45 wt%, Bi 55 wt%)
Simulation universe side length(mm)	870	870
Coolant density ($kg \cdot m^{-3}$)	610	10280
Total burnup ($GWd \cdot t_{HM}^{-1}$)	200	200
Burnup step width ($GWd \cdot t_{HM}^{-1}$)	2.5	2.5
Burnup steps	81	81
Fission rate density ($m^{-3} \cdot s^{-1}$)	$1.32 \cdot 10^{19}$	$1.17 \cdot 10^{19}$

[a] Natural uranium composition.
[b] ^{238}Pu 1.3 wt.%, ^{239}Pu 60.4 wt.%, ^{240}Pu 23.4 wt.%, ^{241}Pu 10.4 wt.%, ^{242}Pu 4.5 wt.%.
[c] C 0.01 wt.%, Ca <0.01 wt.%, Co < 0.03 wt.%, Cr 15.1 wt.%, Cu < 0.05 wt.%, Mn < 2 wt.%, Mo 1.2 wt.%, N < 0.015 wt.%, Ni 15 wt.%, P < 0.015 wt.%, Si 0.4 wt.%, Ti 0.5 wt.%.

Table A2
Specifications of the SCIANTIX simulations for the two fuel/reactor combinations.

Parameter	MOX/SFR	MOX/LBE-FR
Number of history points	81	81
Number of time steps per history point	1000	1000
Irradiation time (h)	120000	106000
Burn-up at discharge (GWd·t_{HM}^{-1})	226	200
Fission rate density (fissions $m^{-3}·s^{-1}$)	$1.32·10^{19}$	$1.17·10^{19}$
Fuel density (kg·m^{-3})	10970	10970
O/M ratio	1.957	1.957

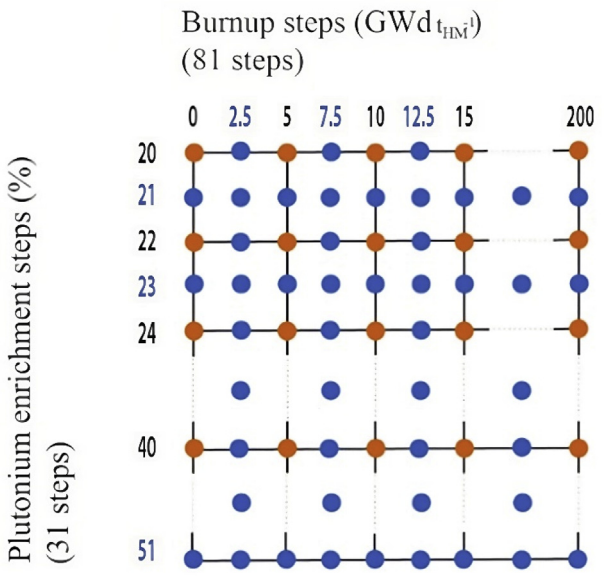

Fig. A1. Burnup/enrichment grid used for verification of the SCIANTIX burnup module against SERPENT (blue, this work; orange, Cechet et al. (2021) [24], i.e., previous version of the burnup module itself).

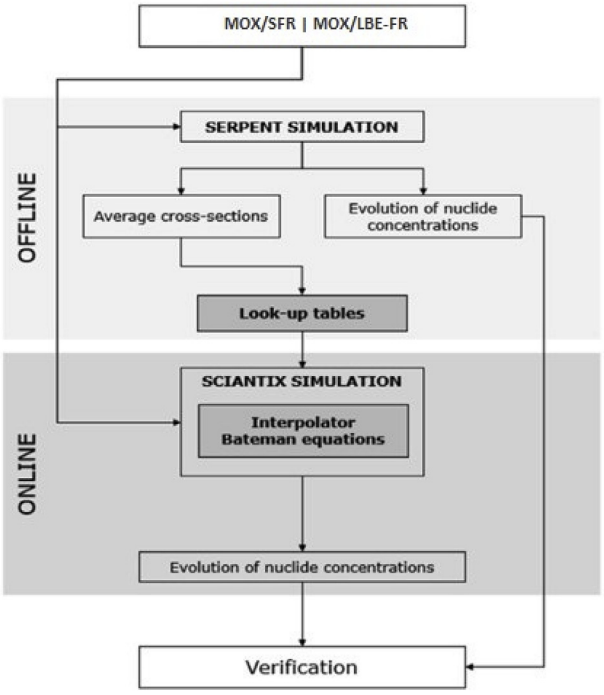

Fig. A3. Standardized methodology applied for the generation of the cross-section look-up table for the corresponding fuel/reactor combination. SERPENT simulations are performed OFFLINE, while the SCIANTIX simulations are performed ONLINE.

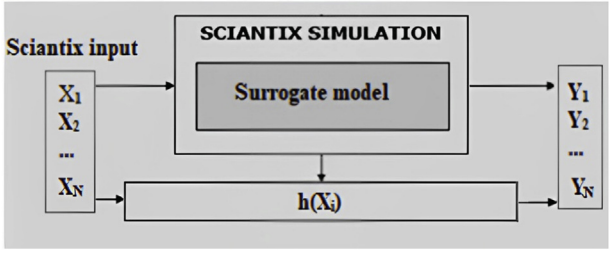

Fig. A.4. Schematic representation of the process of developing a surrogate model for the helium production rate. First, SCIANTIX burnup module was used to obtain a dataset relating the output vector to the input matrix. Secondly, the surrogate model h(**Xi**) was developed based on the training dataset.

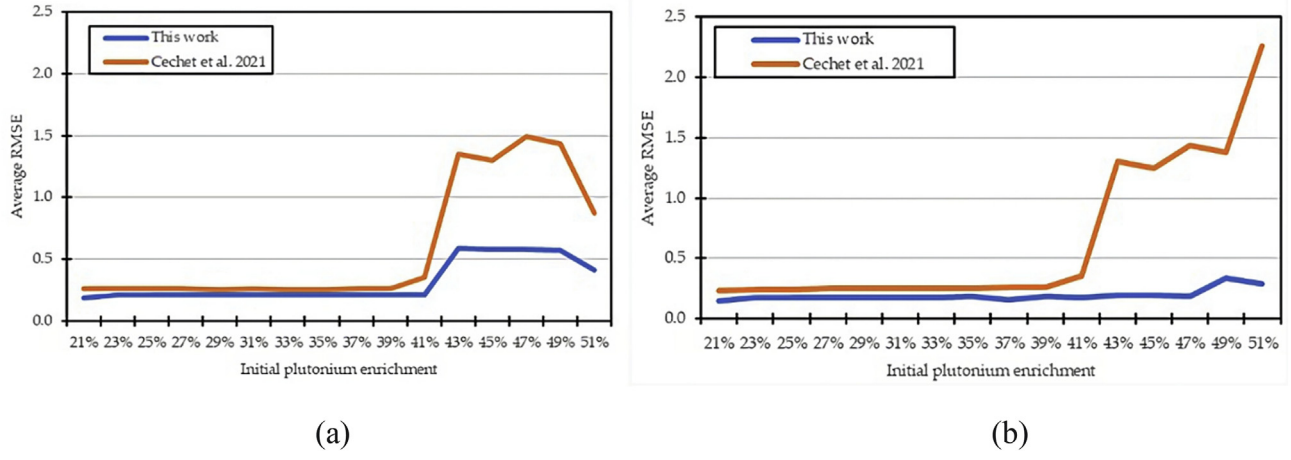

Fig. A2. Comparison of the RMSE (averaged in burnup and on all nuclides) between the SCIANTIX burnup module and SERPENT reference results for the SFR case (a) and for the LBE-FR case (b), as a function of initial plutonium enrichment of the fuel.

References

[1] K. SHIBATA, et al., Japanese evaluated nuclear data library version 3 revision-3: JENDL-3.3, J. Nucl. Sci. Technol. 39 (11) (2002) 1125–1136, https://doi.org/10.1080/18811248.2002.9715303.

[2] M.E. Meek, B.F. Rider, Compilation of Fission Product Yields, Vallecitos Nuclear Center, 1974. United States, 1974. [Online]. Available: https://www.osti.gov/biblio/4279375.

[3] M.J. Bell, origen-2 Code," *ORNL-Tm4397*, Oak Ridge National Laboratories (ORNL), 1973.

[4] D.I. Poston, H.R. Trellue, User's Manual, Version 1.00 for Monteburns, Version 3.01, 1998, https://doi.org/10.2172/307942. United States.

[5] S.M. Bowman, M.D. DeHart, C. V Parks, Validation of SCALE-4 for burnup credit applications, Nucl. Technol. 110 (1) (1995) 53–70.

[6] S. Xia, et al., Development of a molten salt reactor specific depletion code MODEC, Ann. Nucl. Energy 124 (Feb. 2019) 88–97, https://doi.org/10.1016/j.anucene.2018.09.032.

[7] J. de Troullioud de Lanversin, M. Kütt, A. Glaser, ONIX: an open-source depletion code, Ann. Nucl. Energy 151 (Feb. 2021) 107903, https://doi.org/10.1016/j.anucene.2020.107903.

[8] P.K. Romano, N.E. Horelik, B.R. Herman, A.G. Nelson, B. Forget, K. Smith, OpenMC: a state-of-the-art Monte Carlo code for research and development, Ann. Nucl. Energy 82 (2015) 90–97, https://doi.org/10.1016/j.anucene.2014.07.048.

[9] I.R. Birss, Helium production in reactor materials, J. Nucl. Mater. 34 (3) (1970) 241–259.

[10] L.R. Greenwood, A new calculation of thermal neutron damage and helium production in nickel, J. Nucl. Mater. 115 (2–3) (1983) 137–142.

[11] K. Lassmann, TRANSURANUS: a fuel rod analysis code ready for use, J. Nucl. Mater. 188 (1992) 295–302, https://doi.org/10.1016/0022-3115(92)90487-6.

[12] K. Geelhood, W. Luscher, P. Raynaud, I. Porter, FRAPCON-4.0: A Computer Code for the Calculation of Steady-State, Thermal-Mechanical Behavior of Oxide Fuel Rods for High Burnup, 2015.

[13] C. Lee, D. Kim, J. Song, J. Bang, Y. Jung, RAPID model to predict radial burnup distribution in LWR UO 2 fuel, Journal of Nuclear Materials - J NUCL MATER 282 (Dec. 2000) 196–204, https://doi.org/10.1016/S0022-3115(00)00408-6.

[14] S.Y. Kurchatov, V. v Likhanskii, A.A. Sorokin, O. v Khoruzhii, RTOP-code simulation of the radial distribution of heat release and plutonium isotope accumulation in high burnup oxide fuel, Atom. Energy 92 (4) (2002) 349–356.

[15] A. Soba, A. Denis, Simulation with DIONISIO 1.0 of thermal and mechanical pellet-cladding interaction in nuclear fuel rods, J. Nucl. Mater. 374 (Feb. 2008) 32–43, https://doi.org/10.1016/j.jnucmat.2007.06.020.

[16] H. Akie, I. Sato, M. Suzuki, H. Serizawa, Y. Arai, Simple formula to evaluate helium production amount in fast reactor MA-containing MOX fuel and its accuracy, J. Nucl. Sci. Technol. 50 (1) (2013) 107–121.

[17] V.I. Tarasov, E.F. Mitenkova, N. v Novikov, MFPR/R-Aided modeling of hydrogen and helium production in nuclear fuel, Atom. Energy 125 (6) (2019) 370–375, https://doi.org/10.1007/s10512-019-00496-3.

[18] E. Federici, A. Courcelle, P. Blanpain, H. Cognon, Helium Production and Behavior in Nuclear Oxide Fuels during Irradiation in LWR, United States: American Nuclear Society - ANS, La Grange Park (United States), 2007 [Online]. Available: https://www.osti.gov/biblio/21229336.

[19] P. van Uffelen, J. Hales, W. Li, G. Rossiter, R. Williamson, A review of fuel performance modelling, J. Nucl. Mater. 516 (2019) 373–412, https://doi.org/10.1016/j.jnucmat.2018.12.037.

[20] K. Lassmann, The structure of fuel element codes, Nucl. Eng. Des. 57 (1) (1980) 17–39, https://doi.org/10.1016/0029-5493(80)90221-6.

[21] R.L. Williamson, et al., Multidimensional multiphysics simulation of nuclear fuel behavior, J. Nucl. Mater. 423 (1) (2012) 149–163, https://doi.org/10.1016/j.jnucmat.2012.01.012.

[22] J.C. Helton, F.J. Davis, Latin hypercube sampling and the propagation of uncertainty in analyses of complex systems, Reliab. Eng. Syst. Saf. 81 (1) (2003) 23–69, https://doi.org/10.1016/S0951-8320(03)00058-9.

[23] D. Pizzocri, T. Barani, L. Luzzi, SCIANTIX: a new open source multi-scale code for fission gas behaviour modelling designed for nuclear fuel performance codes, J. Nucl. Mater. 532 (Apr. 2020), https://doi.org/10.1016/j.jnucmat.2020.152042.

[24] A. Cechet, et al., A new burn-up module for application in fuel performance calculations targeting the helium production rate in (U,Pu)O2 for fast reactors, Nucl. Eng. Technol. 53 (6) (Jun. 2021) 1893–1908, https://doi.org/10.1016/j.net.2020.12.001.

[25] J. Leppänen, M. Pusa, T. Viitanen, V. Valtavirta, T. Kaltiaisenaho, The Serpent Monte Carlo code: status, development and applications in 2013, Ann. Nucl. Energy 82 (Aug. 2015) 142–150, https://doi.org/10.1016/j.anucene.2014.08.024.

[26] D. Olander, Nuclear fuels – present and future, J. Nucl. Mater. 389 (1) (2009) 1–22, https://doi.org/10.1016/j.jnucmat.2009.01.297.

[27] J.M. Bonnerot, Thermal Properties of Mixed Uranium and Plutonium Oxides, CEA Centre d'Etudes Nucleaires de Cadarache, 1988.

[28] J.J. Carbajo, G.L. Yoder, S.G. Popov, V.K. Ivanov, A review of the thermophysical properties of MOX and UO2 fuels, J. Nucl. Mater. 299 (3) (2001) 181–198, https://doi.org/10.1016/S0022-3115(01)00692-4.

[29] G. Locatelli, M. Mancini, N. Todeschini, Generation IV nuclear reactors: current status and future prospects, Energy Pol. 61 (2013) 1503–1520, https://doi.org/10.1016/j.enpol.2013.06.101.

[30] K. Tasaka, et al., JNDC Nuclear Data Library of Fission Products, second version, Japan Atomic Energy Research Inst., 1990.

[31] S. Altieri, A Burnup Meta-Model for Application in Fuel Performance Codes: Development and Verification for MOX Fuel in Pressurized Water Reactors, MSc Thesis, Politecnico di Milano, 2019.

[32] A. Cechet, Modelling of Helium Behaviour in Oxide Nuclear Fuels for Fuel Performance Analysis, MSc Thesis, Politecnico di Milano, 2020.

[33] M.D. McKay, R.J. Beckman, W.J. Conover, Comparison of three methods for selecting values of input variables in the analysis of output from a computer code, Technometrics 21 (2) (May 1979) 239–245, https://doi.org/10.1080/00401706.1979.10489755.

[34] The MathWorks Inc, MATLAB, Natick, Massachusetts, 2019.

[35] SAS Institute Inc, JMP®, Version 16.1, 2021. Cary, NC.

[36] K. Pearson, X. On the criterion that a given system of deviations from the probable in the case of a correlated system of variables is such that it can be reasonably supposed to have arisen from random sampling, London, Edinburgh Dublin Phil. Mag. J. Sci. 50 (302) (Jul. 1900) 157–175, https://doi.org/10.1080/14786440009463897.

[37] A.S.S.K.B. Glantz, Primer of Applied Regression and Analysis of Variance, McGraw-Hill, 1990.

[38] J. Leppänen, Serpent—a Continuous-Energy Monte Carlo Reactor Physics Burnup Calculation Code, vol. 4, VTT Technical Research Centre of Finland, 2013.